Radiation Physics and Chemistry 155 (2019) 260–264

Contents lists available at ScienceDirect

Radiation Physics and Chemistry

journal homepage: www.elsevier.com/locate/radphyschem

Improvement of Sievert Integration Model in brachytherapy via inverse problems and Artificial Neural Networks

Eriberto O. do Nascimento[a], Lucas N. de Oliveira[a,b], Linda V.E. Caldas[b,*]

[a] Instituto Federal de Educação, Ciência e Tecnologia de Goiás-IFG, Campus Goiânia, 74055-110 Goiânia, GO, Brazil
[b] Instituto de Pesquisas Energéticas e Nucleares, Comissão Nacional de Energia Nuclear-IPEN/CNEN, 05508-000 São Paulo, SP, Brazil

ARTICLE INFO

Keywords:
Brachytherapy
Sievert Integration Model
Artificial Neural Networks
Inverse problems

ABSTRACT

Increasing the radial distance, the accuracy of the Sievert Integration Model (SIM) decreases in a nonlinear manner, adding errors up of 10% into the dose rate calculations; a similar fact occurs to the 2D anisotropy function where the errors may achieve 30% as already was related. For that reason, this paper sought an innovative approach to optimize the error variance and its biases of dose rate calculations around a Nucletron brachytherapy source of ^{192}Ir from 0 to 10 cm taken in the radial distance, using an improved SIM through a hybrid coupling of Artificial Neural Networks (ANNs) and Inverse Problem Theory (IPT). Since the traditional approach relies into the use of a small data set of dose rate, the ANNs generalized these doses, making possible to search more broadly optimum parameters to SIM using the IPT. The results showed excellent accuracy evaluated with the Root Mean Square Percentage Error (RMSPE). In conclusion, the low RMSPE values indicate that the methodology is consistent, showing an excellent agreement with the state of art of dosimetric measurement techniques.

1. Introduction

The Sievert Integration Method (SIM) relies as one of the most important analytical modelling techniques in the radiation physics with direct applications in dosimetric fields (Williamson et al., 1983). Thus, this importance has had established since the 20th century when the lack of computers boosted the analytical methods to a highlighted place of significance, as example, many tables of daily routine of Brachytherapy treatments used the Sievert model to calculate the equivalent doses. However, few attempts had tried to improve the analytical Sievert method, since other methods like Monte Carlo (MC) appeal to be a more manageable and easy to perform calculations.

Contrary to this, several researchers had shown that the SIM can describe the accurate dose rate distribution for many brachytherapy sources, and the small computational execution time and the easy to perform implementations are the core advantages compared with the traditional Monte Carlo codes (Pantelis et al., 2002a, 2002b; Williamson, 1996).

Williamson and Li (1995) and Karaiskos et al. (2000) pointed already out that with the increase of the radial distance, the accuracy of SIM decreases in a non-linear manner, adding errors of 10% or larger for the dose rate calculations. For the anisotropic function, for a range of angles varying from 14 to 30 degrees, the errors can achieve 30% and 26%. For that reason, this work aims to minimize and dissipate these errors over the range from 0 to 10 cm.

Therefore, Artificial Neural Networks (ANNs) and non-linear optimization methods are gaining expressive applications on radiation dosimetry. Numerous papers have tried to use the classification, prediction, clustering and universal approximation features of neural nets, to identify tumors (cancers) in the early stages of development or even trying to predict the probability of cancer appearance as a function of the behavioral and historical records of previous diseases (Álvarez et al., 2010).

Nevertheless, these applications are not exhaustive to the previous cited ones; this paper brings a new kind of use of the ANNs. It will be used to improve the well consolidated analytical methods through a hydric coupling between the experimental and simulated data, used in the references protocols, regulated under the Task Group Activities. These improvements consisted on the updates of the modelling equations, using the state of art experimental measurements to attach a more accurate model, and then updating the equations used in brachytherapy sources.

2. Methods

To improve the SIM, seeking for more accuracy and error

* Corresponding author.
E-mail address: lcaldas@ipen.br (L.V.E. Caldas).

https://doi.org/10.1016/j.radphyschem.2018.05.024
Received 27 July 2017; Received in revised form 26 April 2018; Accepted 22 May 2018
Available online 26 May 2018
0969-806X/

dissipation towards larger radial distances, this work was structured into four main parts, implemented in a straightforward manner, showing the motivations in each section to use the models.

2.1. Consensus data set

There are tremendous efforts by the national politics and international regulatory agencies to get standards to the measurements procedures and data visualization representation in radiation treatments. These efforts are linked, in this work, to the contribution of the American Association of Physics in Medicine (AAPM) on its Task Group No. 43 (AAPM TG-43), and its update (AAPM TG-43U1) and supplementation (AAPM TG-43U1S1) (Rivard et al., 2004, 2007) where mathematical equations allowed researchers to get standard results to their experimental or simulated results in front of benchmarked protocols. Those protocols facilitate the comparison among different data sets.

The TG-43 formalism defined expressions for brachytherapy source, around water, such as the air-kerma strength, geometry function, radial dose function and the 2D anisotropy function. These expressions apply for cylindrically symmetric dose distributions along the longitudinal axes of the sources.

After the proper definition of the TG-43 formalism, the reference data of the dose rate was collected to measure the quality of the SIM model against this reference. Ever since, a previous version of the Sievert Method compared its accuracy with different data sets, like did the models made by Williamson and Li (1995) and Karaiskos et al. (2000), that compared the quality of their models with experimental data in the case of Karaiskos et al. (2000) and with simulated data through Monte Carlo, as did Williamson and Li (1995). In this work, these same models were evaluated, comparing them with a third data source, preventing then a biased analysis of which model was the best to modelling the dose rate distribution with greater accuracy.

Then, the AAPM Consensus, supplied by Perez-Calatayud et al. (2012) served as the reference dimensional (2D) dose rate distribution for the Nucletron Micro-Seletron source data set and geometrical features, like nuclei diameter and length as so materials and their disposition on the source model. Initially the ^{192}Ir sources came from different manufactures; it includes the Nucletron and Varian sources. The Monte Carlo (MC) calculations presented at the AAPM Consensus data were calculated using the EGSnrc user-code (Perez-Calatayud et al., 2012).

2.2. Mathematical models

Williamson and Li (1995) proposed an approach to implement an analytical solution of the Sievert Equation model, dividing the original model into two components (the scatter and primary dose rate); this setup was called the isotropic scatter model. They were applied successfully in the High Dose Rate (HDR) sources of ^{125}Ir, ^{169}Yb and ^{192}Ir with clinical acceptable errors. Then, Karaiskos et al. (2000) proposed Eq. (1), which combines the scattering and primary dose rate function (SPR), into a single equation; they also proposed to use a correction factor into the SPR function. Karaiskos et al. (2000) affirmed that their model required few inputs to its implementation and it was computationally efficient in terms of time execution.

$$\dot{D}(r,\theta) = \frac{1}{N} S_k \overline{(\mu_{en}/\rho)}_{air}^{water} \cdot \sum_{i=1}^{N} \left[\left(\frac{\exp(\mu_s s_i - \mu_f f_i - \mu_w w_i)}{F(r_c)} + \exp(-\mu_w r) \cdot \mathrm{SPR}(r) \cdot \mathrm{C}(r,\theta) \right) r_i^{-2} \right] \quad (1)$$

where N is a finite number of small segments in which the active length L is discretized; S_k is the air-kerma strength; μ_s, μ_f and μ_w are the effective filtration coefficients of the source, encapsulation and the water medium respectively. SPR(r) is the scatter to primary dose rate ratio: Eq. (2); C(r, θ) is a correction factor: Eq. (3); r is the radial distance and θ the angular displacement to the point of calculation; r_i is the distance between the i^{th} segment in the N_i segment in the center of the source relative from the measurement point. The s_i, f_i and w_i are the traveled distances of photon from the mid of the source center, encapsulation

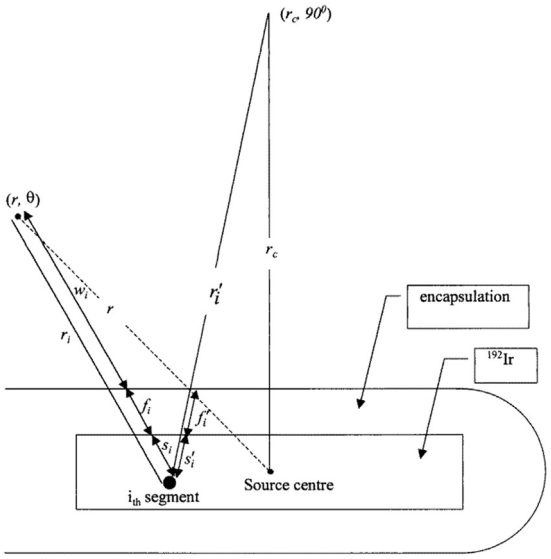

Fig. 1. Schematic representation of the SIM method, this figure shows the reference distances presented at Eq. (1). Adapted from Karaiskos et al. (2000).

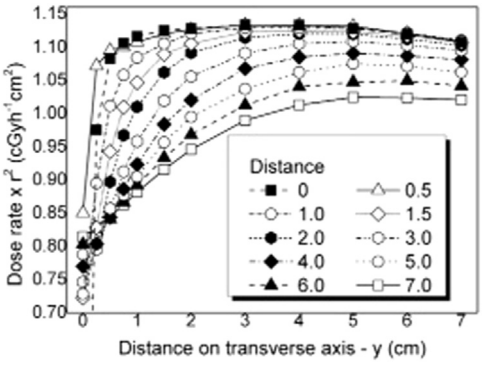

Fig. 2. Distance on transverse axis – y versus the dose rate multiplied by squared radial distance. This figure shows the nonlinear mapping of the doses, used as the input data to the trained ANN.

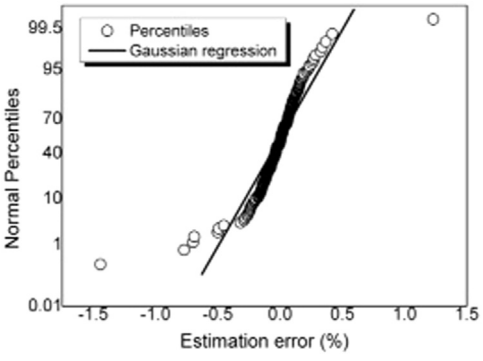

Fig. 3. Normal percentiles versus estimation error. This figure shows the estimation error using an ANN to approximate the dose rate from the Consensus data set. The samples are the dose rate multiplied by the squared radial distance as a function of the z - and y - coordinates taken from the Consensus data set.

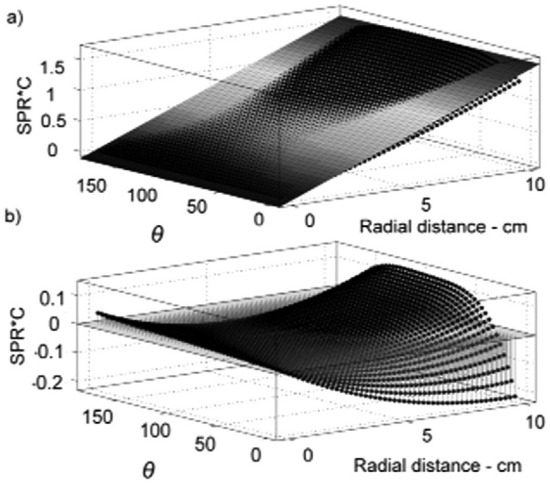

Fig. 4. Comparison between two surfaces: a) Product of the SPR and C expressions originally proposed in Eq. (1) and the flat plan of Eq. (7). b) Residual difference of the SPRC product relative to the plan surface, highlighting the distortions presented at extreme angles.

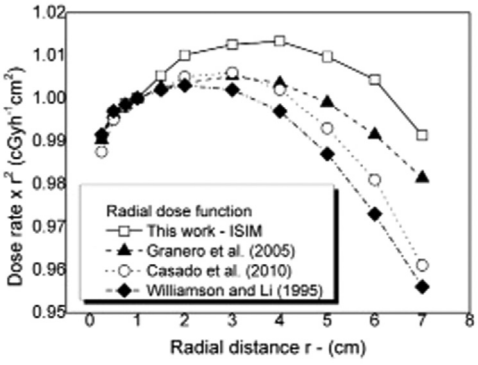

Fig. 5. Comparison of the radial dose function plot from different methods. This figure captured the result of ISIM method, showing a good agreement with the literature data.

material and the calculation point respectively, $F(r_c)$ is the normalization of dose: see Eq. (4); $(\overline{\mu_{en}/\rho})_{air}^{water}$ is the ratio mass-energy absorption coefficient.

$$\mathrm{SPR}(r) = 0.135r + 0.003r^2 \tag{2}$$

$$\mathrm{C}(r, \theta) = 1 - (3x10^{-9}) \times (\theta - 90^{\circ})^4 \tag{3}$$

$$F(r_c) = \frac{1}{N} \bullet \sum_{i=1}^{N} [\exp(-\mu_s s_i' - \mu_f f_i')/r_i'^2] \tag{4}$$

where s_i' , f_i' and $r_i'^2$ are the distances within source and encapsulation material from the i^{th} segment to the calibration distance r_c. Fig. 1 shows the distances defined in Eqs. (1) and (4). The computational solution of Eq. (1) required the construction of a virtual source model with the dimensions of the mHDR Nucletron Selectron v1 and its geometrical features. The Matlab© software serves as the computational developing environmental to the model.

However, Karaiskos et al. (2000) and Pantelis et al. (2002a, 2002b) showed that with the increase of radial distance the accuracy decreases in a non-linear manner, adding errors of 10% or larger for the dose rate calculations. For the anisotropic function, for a range of angles varying from 14 to 30 degrees the errors can achieve 30% and 26% as related, indicating consequently that the SIM model, Eq. (1), needed adjustments on these improvements. Therefore, these improvements can be achieved using the Artificial Neural Networks and the Inverse Problem methodology, which are described in Sections 2.3 and 2.4 respectively.

2.3. Artificial Neural Networks

In this work, the ANNs performed a multidimensional approximation on the dose rate data set published as the Consensus data from the AAPM report, for the Nucletron source ^{192}Ir. A homemade code used the Matlab toolbox of Neural Networks, the 'nntool' (Mark et al., 2014) to model the network topology.

The input data were the Cartesian coordinates (z, y) for the distances along the source representing the z-axis and the distance from away the source that stands for the y-axis. The z-axis was delimited from − 7–7 cm, while the y-axis from 0 cm to 7 cm; the output was the dose rate, a function of the coordinate (z, y). The two hidden layers were set to have twenty neurons on each one; the activation functions in the hidden layers were set as the sigmoidal function, and the output layer the linear function. Then, the ANNs were trained in a supervised scheme, using the error back propagation algorithm optimized by the Levenberg-Marquardt Training (Hagan and Menhaj, 1994), applied on a Multilayer Perceptron (MLP) (Russell and Norvig, 1995), architecture, resulting in a MLP 2–20-20-1.

Since the dose rate distribution relies on a certain type of Gaussian distribution, in the nearest region of the seed nuclei the dose tends to high values, such as 3.18×10^{8} Gy at the origin (0, 0) cm, contrary, lower doses for larger radial distances as 2.20×10^{-4} Gy at 10 cm which is approximately in the (−7, 7) cm coordinate position. Consequently, a pre-processing was required to eliminate possible singularities and to improve the ANN training performance, so the input data were scaled into the range of − 1 to + 1 in non-dimensionally units; the output was first scaled into a non-linear mapping from 0 to 1 and then to a linear mapping from − 1–1 a-dimensionally units. The non-linear mapping was performed by the multiplication of the dose rate at the point (z, y) by its squared radial distance, of z and y, calculated as the bi-dimensional Euclidean distance, $r = (z^2 + y^2)^{1/2}$, where "r" is the radial distance.

After defined the topology and the training phase, the input data were set in the training, validation and tests groups, in the 80%, 10% and 10% proportion respectively. The data were allocated randomly on these three groups regarding its proportion from the inputs and output pairs. The performance training function was set as the Mean Squared Error (MSE) and the Pearson R^2 correlation coefficient (Mark et al., 2014); both of these functions were evaluated between the target value and the estimated output obtained after the training. The stop training criterions were defined: maximum 1000 numbers of epochs; limit time of training of 360 s; if the incremental change in the gradient was smaller than 1.00×10^{-10}; and finally if the performance function MSE hit the 1.00×10^{-10} value the training phase stops.

2.4. Sv improvement

The traditionally employed techniques to error minimization between two different systems with the same output is to apply a fitting procedure, to adjust one in front of another. The non-linear regression plays an important role when it comes to the improvement of the accuracy; this approach to get the constituent parameters from the observations on a model function passes through a Nonlinear Least Squared Fitting procedure, which relies on an optimization problem and on an Inverse Problem Theory (IPT) method perspective (Edwin and Stanislaw, 2013). At this work, the cost function, Eq. (5), performs an evaluation on the residual value between the set of the observation and the set of the estimated-based model. Williamson (1996) applied a similar procedure to the ^{60}Co source, to get two parameters for the filtration coefficients based on the MC simulations.

However, Williamson (1996) obtained its results from a small data set of the discrete tabulated results following the TG43 formalism representation. In the present work, the ANNs proved to be an alternative

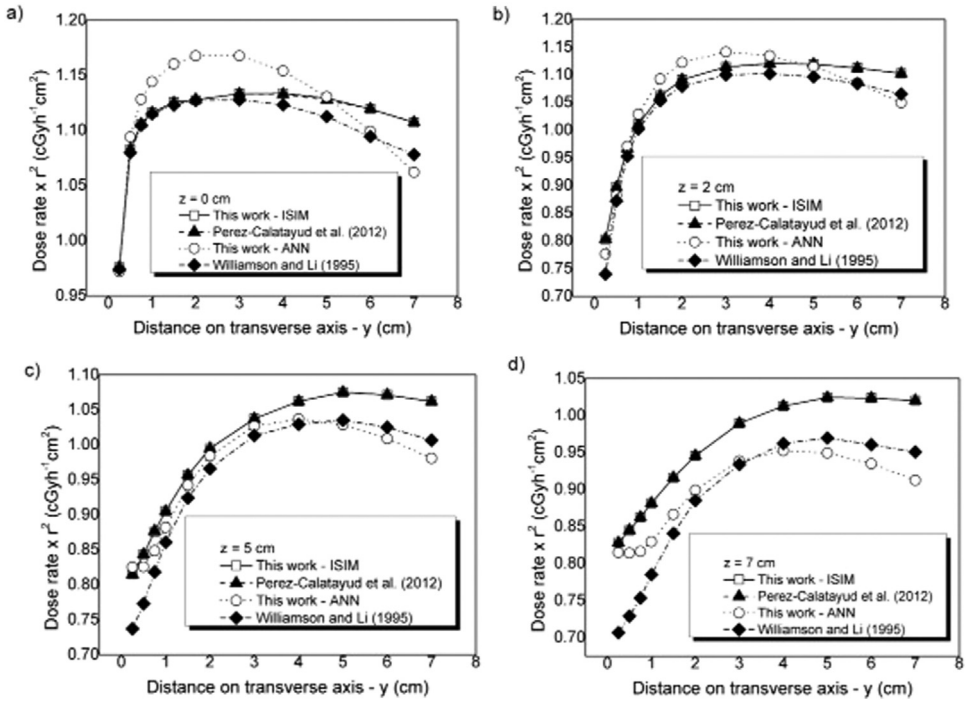

Fig. 6. Model response of the proposed ISIM and comparison with the literature data using MC techniques, evaluated at: a) z = 0 cm, b) z = 2 cm, c) z = 5 cm and d) z = 7 cm.

to generalize the results from the AAPM Consensus data (Perez-Calatayud et al., 2012), which contain a larger range of doses and distances, then allowing the search for better parameters for Eq. (1).

$$\%\sigma_{RMSPE}(\mu_1, \mu_2) = 100 \cdot \sqrt{\sum_{i=1}^{N} \left(\frac{[\dot{D}(r, \theta; \mu_1, \mu_2)/S_k]_{ISIM}}{([\dot{D}(r, \theta)/S_k]_{EGSnrc})_{ANN}} - 1 \right)^2 / N} \quad (5)$$

$$(\hat{\mu}_1, \hat{\mu}_2) = arg\ min\{\%\sigma_{RMSPE}(\mu_1, \mu_2)\} \quad (6)$$

where $\%\sigma_{RMSPE}(\mu_1, \mu_2)$ is the cost function, taken as the Root Mean Squared Percentage Error (RMSPE), μ_1 and μ_2 are the parameters under optimization, $([\dot{D}(r, \theta)/S_k]_{EGSnrc})_{ANN}$ is the ANN approximation of the MC code EGSnrc, presented in the AAPM Consensus data [9]; $(\hat{\mu}_1, \hat{\mu}_2)$ are the estimated parameters that will minimize the error, Eq. (5). The expression $[\dot{D}(r, \theta; \mu_1, \mu_2)/S_k]_{ISIM}$ stands for the Improved Sievert Integration Model (ISIM) that was achieved by substituting the product of SPR and C functions at the Eq. (1) by the expression at Eq. (7):

$$CF(r, \theta) = \mu_1 r + \mu_2 \theta \quad (7)$$

where $CF(r, \theta)$ is the Correction Function.

The computational implementations were performed in Matlab© software, version R2014a, applying the inline functions of the optimization toolbox, optimtool (Matlab, 2014). The adjustment parameters μ_1 and μ_2 used the Levenberg-Marquardt algorithm and the Trust-Region Reflection method was configured according to the Matlab© defaults.

3. Results and discussion

Fig. 2 shows the dose rate per unit air kerma versus the radial distance for the mHDR Nucletron Selectron v1. These data served as the reference data from the AAPM, as set in Section 2.1. In addition, Fig. 2 shows the non-linear mapping performed on the dose rate; it is possible to verify that any singularities related with high dose rates at small and large distances were dissipated. Consequently, with the singularities disappearance the training performance of the ANN was greatly upgraded, then collaborating to find a final ISIM model with clinical acceptable errors as discussed at the Section 2.3.

Fig. 3 shows the approximation error performed by the ANN generalization on the (z-axis, y-axis; Dose rate) data from the nonlinear mapping. The approximation error was the relative percentage error with the reference data from the AAPM MC simulated data (Perez-Calatayud et al., 2012). The statistical parameters of this error were: standard deviation value of 0.2035%, mean value of − 0.017%, minimum error of − 1.4419% and maximum error of 1.2302%; these qualifiers prove that the ANN performed an excellent approximation, due to its small error descriptors, with low standard deviation and mean value.

Fig. 4a reveals, accordingly with was stated on Section 2.4, that the ISIM method attached its improvement relative with the substitution of the SPR and C product, on Eq. (1), by only a new surface, expressed by Eq. (7). Therefore, Fig. 4b shows only extreme angles, from 0 to 10 degrees and from 170° to 180° of the SPR and C product, curved the surface response. In relation to the new Eq. (7), this modification of curvature at the extremes angles, leaving only a flat plan, shall not be taken.

With the good results of the ANN approximation, the improvement of the SIM to the ISIM was straightforward, with the implementation of the IVT through Eq. (5), to adjust the optimal parameters of Eq. (7) that were obtained as $\mu_1 = 0.1647$ and $\mu_2 = 6.4499$. Then, to certify the accuracy of the obtained results from the new ISIM modelling equations, the TG-43 formalism was evaluated using other sources besides mHDR Nucletron Selectron v1; the sources were BEBIG Ir-192 HDR, Varisource VS2000 HDR just adjusting the filtration coefficients.

Fig. 5 shows the Radial Dose Function plot against the results from the literature data of the BEBIG ^{192}Ir HDR (Granero et al., 2005), Varisource VS2000 HDR (Casado et al., 2010) and microSelectron HDR (Perez-Calatayud et al., 2012). The ISIM method was performed with a RMSPE of 3.29% when compared to the results presented by Williamson and Li (1995), indicating excellent results, since there are no significant discrepancies at the modelled curves.

In the Fig. 6a complete inspection into the radial distance from 0 up to 10 cm was made; these graph prove that the proposed methodology successfully dissipated and mitigated the higher errors as the radial

distance increase. In summary, the RMSPE value for these doses taken at the distance of z (along the source) in the range of 0, 0.5, 1, 2, 3, 4, 5, 6 and 7 cm were respectively 2.54%, 2.48%, 1.66%, 2.16%, 2.71%, 2.57%, 2.75%, 2.65% and 2.74%.

4. Conclusions

A new improved model for the Sievert Integration was obtained using a hybrid couple between neural nets and the inverse problem theory. The ANN successfully approximated the dose rate distribution along the mHDR Nucletron Selectron v1 source with maximum error of 1.21%. The ISIM method from the range of 0–10 cm of radial distance regularized the approximation errors, measured with RMSPE error of 2.47 ± 0.35%. The radial dose rate calculation using the ANN and the ISIM method benchmarked against the TG-43 formalism showed excellent results with an approximation error of only 3.29%. These results show that the ISIM may be a promising tool for dosimetry evaluations with clinical acceptable errors.

Acknowledgments

This research was supported in part by the Brazilian agencies: CNPq, under Grants Nos. 165466/2015-4, 151013/2014-4, and 301335/2016-8, FAPESP and MCTI, Brazil (Project INCT for Radiation Metrology in Medicine), for partial financial support.

References

Álvarez, L., de Cos Juez, F., Sánchez, F., Álvarez, J., 2010. Artificial neural networks applied to cancer detection in a breast screening programme. Math. Comput. Model. 56, 983–991.

Casado, F.J., García-Pareja, S., Cenizo, E., Mateo, B., Bodineau, C., Galán, P., 2010. Dosimetric characterization of an ^{192}Ir brachytherapy source with the Monte Carlo code PENELOPE. Med. Phys. 26, 132–139.

Edwin, C., Stanislaw, Z., 2013. An Introduction to Optimization, fourth ed. John Wiley & Sons, New York.

Granero, D., Pérez-Calatayud, J., Ballester, F., 2005. Monte Carlo calculation of the TG-43 dosimetric parameters of a new BEBIG ^{192}Ir HDR source. Radiother. Oncol. 76, 79–85.

Hagan, T., Menhaj, M., 1994. Training feed forward networks with the Marquardt algorithm. IEEE Trans. Neural Netw. 5, 989–993.

Karaiskos, P., Angelopoulos, A., Baras, P., Rozaki-Mavrouli, H., Sandilos, P., Vlachos, L., Sakelliou, Y., 2000. Dose rate calculations around ^{192}Ir brachytherapy sources using a Sievert integration model. Phys. Med. Biol. 45, 383–398.

Mark, B., Hagan, T., Demuth, H., 2014. Neural Network Toolbox. Neural Network Toolbox – Version R2014a. The MathWorks. Inc., USA, pp. 435.

Matlab, 2014. Optimization Toolbox™ User's Guide (Release 2014b). The MathWorks, Inc., USA.

Pantelis, E., Baltas, D., Dardoufas, K., Karaiskos, P., Papagiannis, P., Rosak, H., Sakelliou, L., 2002a. On the dosimetric accuracy of a Sievert integration model in the proximity of ^{192}Ir HDR sources. Int. J. Radiat. Oncol. 53, 1071–1084.

Pantelis, E., Baltas, D., Dardoufas, K., Karaiskos, P., Papagiannis, P., Rosaki-Mavrouli, H., Sakelliou, L., 2002b. On the dosimetric accuracy of a Sievert integration model in the proximity of ^{192}Ir HDR sources. Int. J. Radiat. Oncol. Biol. Phys. 53, 1071–1084.

Perez-Calatayud, J., Ballester, F., Das, R.K., DeWerd, L.A., Ibbott, G.S., Meigooni, A.S., Williamson, J., 2012. Dose calculation for photon-emitting brachytherapy sources with average energy higher than 50 keV: report of the AAPM and ESTRO. Med. Phys. 39, 2904–2929.

Rivard, M.J., Butler, W.M., DeWerd, L.A., Huq, M.S., Ibbott, G.S., Meigooni, A.S., Melhus, C.S., Mitch, M.G., Nath, R., Williamson, J., 2007. Supplement to the 2004 update of the AAPM Task Group No. 43 Report. Med. Phys. 34, 2187–2205.

Rivard, M., Coursey, B., DeWerd, L., Hanson, W., Saiful Huq, M., Ibbott, G., Mitch, M., Nath, R., Williamson, J., 2004. Update of AAPM Task Group No. 43 Report: a revised AAPM protocol for brachytherapy dose calculations. Med. Phys. 31, 633–674.

Russell, J., Norvig, P., 1995. Artificial Intelligence – A Modern Approach, first ed. Prentice Hall, New Jersey, USA.

Williamson, J., 1996. The Sievert integral revisited: evaluation and extension to ^{125}I, ^{169}Yb, and ^{192}Ir brachytherapy sources. Int J. Radiat. Oncol. 36, 1239–1250.

Williamson, J., Li, Z., 1995. Monte Carlo aided dosimetry of the microselectron pulsed and high dose-rate ^{192}Ir sources. Med. Phys. 22, 809–819.

Williamson, J., Morin, L., Khan, F., 1983. Monte Carlo evaluation of the Sievert integral for brachytherapy dosimetry. Phys. Med. Biol. 28, 1021–1032.